

Equilibrium and fractal-like kinetic studies of the sorption of acid and basic dyes onto watermelon shell (*Citrullus vulgaris*)

Emmanuel C. Chigbundu · Kayode O. Adebowale

Received: 16 February 2017 / Accepted: 7 September 2017 / Published online: 16 September 2017
© Springer Science+Business Media B.V. 2017

Abstract In the present study, batch experiments were used to determine adsorption characteristics of Watermelon Shell Biosorbent (WSB) for the uptake of anionic and cationic dyes from aqueous solution. Various factors such as initial dye concentration, adsorbent dosage, pH, contact time and temperature were systematically investigated and discussed. WSB was characterized by Scanning Electron Microscopy, Energy Dispersive X-ray Spectroscopy and Fourier Transform Infrared Spectroscopy. The adsorption kinetics was best described by Elovich and Diffusion-Chemosorption models for Basic red 2 (BR2) (cationic dye) and Orange G (OG) (anionic dye) respectively. However, the fractional time index “ α ” and non-integer “ n ” order by Fractal-like pseudo-first order kinetic affirmed that the mechanism of interaction of both dyes with WSB was by chemical reaction. The applicability of four adsorption isotherm models for the present system was tested. The equilibrium data were found to be well represented by the Extended Langmuir isotherm equation. The monolayer adsorption capacity of WSB for BR2 and OG adsorption was found to be 125 and 27 mg/g,

respectively. The effect of temperature on the adsorption process was also investigated and the values of thermodynamic parameters ΔG° , ΔH° and ΔS° revealed that the adsorption system was spontaneous.

Keywords Thermodynamics · Fractal-like kinetics · Biosorbent · Watermelon shell · Orange G · Basic red 2 · Isotherms

Introduction

Wastewater generated by the textile, paper, carpet, paint. And printing industries often contains high concentrations of coloured effluent resulting from the use of dyes. Due to their complex structure and synthetic origins, dyes are non-biodegradable. Hence, getting rid of dyes from wastewater or the aquatic environment has attracted an urgent attention. They are built to be stable to pH, light irradiation and heat thereby posing a serious threat to human/animal health which is not only limited to themselves but may be passed on to future generation by the way of genetic mutation, birth defects, inherited diseases and so on (Suteu et al. 2009; Zaharia et al. 2009). Several physical and chemical processes has been applied which includes ion exchange, precipitation, electro-dialysis, adsorption, filtration, coagulation, oxidation and membrane separation.

E. C. Chigbundu (✉) · K. O. Adebowale
Department of Chemistry, Faculty of Sciences, University of Ibadan, Ibadan, Oyo State, Nigeria
e-mail: emmachij@yahoo.com

E. C. Chigbundu
Department of Chemical and Food Sciences, Bells University of Technology, Ota, Ogun State, Nigeria

However, adsorption is known to be one of the most effective physical techniques to eliminate dyes from wastewater (Omorieg et al. 2012, 2014; Ogbodu et al. 2015; Yang et al. 2015; Rashid et al. 2016; Tahir et al. 2016). Adsorption has advantages over other techniques in the sense that the design is simple, sludge-free and can involve low investment in terms of both the initial costs and land. Commercial activated carbon has been studied as one of the best and successful adsorbent for several years due to its great specific surface area and pore structure but it is expensive (Depci et al. 2012). To overcome this disadvantage, focus has been on processes that apply low cost adsorbent as evidenced by increased number of literature reports in recent years (Barka et al. 2010; Kanawade and Gaikwad 2011; Omorieg et al. 2012, 2014; Unuabonah et al. 2015).

Many agricultural byproducts and wastes have been applied as biosorbents in recent studies, some of which includes, shells of hazelnut and almond (Bulut and Tez 2007), rice straw (Hameed and El-Khaiary 2008), garlic peel (Hameed and Ahamad 2009), mango peel (Iqbal et al. 2009), mungbean husk (Saeed et al. 2009), orange peel (Gupta and Nayak 2012; Lashee et al. 2012), Watermelon shell (Banerjee et al. 2012), Eucalyptus seeds (Kiruba et al. 2014), Solanum melon-Gena leaf powder (Yuvaraja et al. 2014), *Cedrela odorata* seed waste (Babalola et al. 2016a, b), *Eriobotrya Japonica* seed (Mushtaq et al. 2016) and different low cost adsorbents (Bhattacharya et al. 2008; Gupta et al. 2005).

The development of agricultural by-product with good adsorption capacities may result in economics of scale for water treatment especially in industries local to the production of such by products (Paraskeva et al. 2008). The study of adsorption capacity using agricultural waste for wastewater treatment is significant as it provides valuable insights into potential and applicability of a bio-adsorbent (biosorbent) for the uptake of aquatic pollutant especially dyes. Watermelon shell is low cost because it is available and abundant. As an agricultural waste the shell is either thrown away after the inner part is consumed as trash or abandoned or incinerated. According to Lakshmi-pathy and Sarada (2013) as referred to in Husein et al. (2017), Watermelon rind/shell consists mainly of pectin, cellulose, proteins and carotenoids. These polymers are rich in functional groups such as

hydroxyl (cellulose), carboxylic (pectin) and amine (proteins) (Husein et al. 2017).

Anionic dyes are water soluble dyes applied to nylon, wool, silk and modified acrylics while cationic dyes produces bright shades on wool, orlon, cotton and rayon. However Cationic dyes are more toxic than anionic dyes (Nandi et al. 2009). Therefore it is the aim of this study to investigate the applicability, potentiality or effectiveness of Watermelon Shell as Biosorbent (WSB) for the removal of cationic compared to the uptake of anionic dye, from aqueous solution. Batch adsorption process with respect to the influence of some operating conditions such as initial dye concentration, pH, adsorbent dosage, contact time and temperature will be applied. The fitting of the experimental data to Kinetic and equilibrium Isotherm model equations were also explored to be able to evaluate the rate and capacity at which the dye pollutants are removed from aqueous solutions by WSB.

Materials and methods

Materials

Watermelon Shell waste was collected before disposal from fruits and vegetables stores at a local market in Ogun state Nigeria. They were washed repeatedly with distilled water to remove dust and other impurities. The shells were then kept in hot air oven at 333–343 K for several hours to dry. The dried shells were then pulverized into fine powder by grinding in a mechanical grinder. Afterwards, the fine powder obtained was soaked and washed with distilled deionized water until the brownish colouration of the filtrate became clear and a clean water filtrate was obtained. The washed powdered sample was re-dried and sieved to achieve a biosorbent with particle size of 150 μm . It was preserved in an air tight glass bottles and labelled Watermelon Shell Biosorbent (WSB) for adsorption.

The Basic and Acid dyes used in this study were Safranin-O, a cationic dye also known as Basic red 2 (BR2), and Orange G (OG) an anionic dye respectively, supplied by Sigma Aldrich and was used without further purification. The chemical structures of the dyes are shown in Fig. 1 while the molecular and other physical properties of these dyes are shown in Table 1.

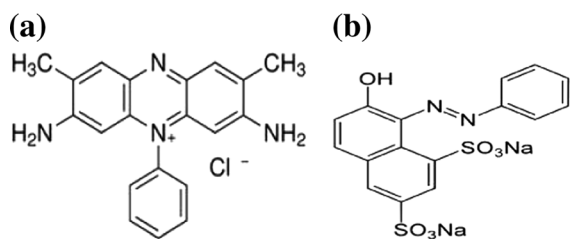


Fig. 1 The chemical structures of **a** Basic red 2 (BR2) and **b** Orange G (OG)

Methods

Stock solutions were prepared by dissolving BR2 and OG dyes in distilled de-ionized water at desired high concentrations in mg/L in two different amber bottles from which lower concentrations were prepared by dilution. A standard calibration curve was plotted and a linear correlation was established between the dye concentrations and their absorbances at individual dyes wavelengths (Table 1). Biosorption of BR2 and OG dyes from aqueous solutions onto WSB was investigated by batch process and the amount of dye removed was calculated as the difference between initial and final dye concentrations. This was determined from their absorbances characteristics in the UV–visible range. A spectrophotometer (Surgifriend SM7504 UV/visible 911) was used for the experiments. The biosorption capacity of WSB was calculated using the expression;

$$qe = \frac{(C_o - C_e) \times V}{W} \quad (1)$$

Table 1 Physicochemical characteristics of WSB and facts on Safranin-O (BR2) and Orange G (OG)

Parameter	Safranin-O	Orange G	WSB
Moisture content	–	–	5.97%
Loss on ignition	–	–	98.97%
Bulk density	–	–	0.28 g/cm ³
pH _{PZC}	–	–	5.45
C.I.	50,240	16,230	–
Colour	Redish	Yellowish	–
Dye content	80%	80%	–
Formula	C ₂₀ H ₁₉ N ₄ Cl	C ₁₆ H ₁₀ N ₂ Na ₂ O ₇ S ₂	–
Molecular weight (FW)	350.85 gmol ⁻¹	452.38 gmol ⁻¹	–
pKa	5.28	–	–
Valence	+1	–1	–
λ _{max}	520 nm	480 nm	–

where C_0 (mg/L) and C_e (mg/L) are the initial and equilibrium concentrations of the dye in solution, respectively, V (L) the volume of the solution and W (g) the weight of the dried watermelon shell biosorbent (WSB) used.

Physicochemical characterization of WSB

WSB was characterized to determine some properties like Bulk density, loss on ignition and moisture Content in accordance with Oladoja and Aliu (2009) method. The microstructural study of WSB was investigated using scanning electron microscope (SEM) (Quanta 200 Model, USA) combined with an energy dispersive X-ray (EDX) spectroscopy. The FTIR spectra of WSB (before and after sorption of dye) recorded on a SHIMADZU Fourier Transform Infrared spectrometer using KBr were used to determine the vibrational frequency changes of the functional groups on the biosorbents.

The Point of Zero Charge (PZC) was determined using the (modified) solid addition method by Oladoja and Aliu (2008). 45 mL of 0.1 M, KNO₃ solution was transferred into series of 100 mL conical flasks. The values of the pH of the solutions in each flask were roughly adjusted from 2 to 10 by adding few drops of either 0.1 M HNO₃ or KOH. The total volume of the solution in each flask was made to 50 mL by adding few more of 0.1 M KNO₃ solution after which 0.5 g WSB was added to each flask and securely capped, immediately. The suspension was then manually agitated intermittently for a period of at least 24 h

and the final values of the pH of the supernatant were noted. The initial (pH_i) values were plotted against the final (pH_f) values. The point of intersection of the resulting curve is the point at which pH gave the Point of Zero Charge.

Adsorption experiment

The effect of pH on the removal performance of the WSB was examined at pH values between 2.0 and 11.0 (adjusted by the addition of few drops of dilute HCl or NaOH solutions).

The biosorption capacity of WSB was investigated by biosorbent dose variation. This was carried out by dispersing between 0.007–0.5 g WSB samples into 20 ml solution of BR2 and OG dyes aqueous solution at an initial dye concentration of 140 mg/l. Both dyes concentration was varied while maintaining a constant mass of WSB to determine the biosorption equilibrium capacity. The equilibrium data were fitted to Langmuir, Freundlich, Extended Langmuir and Exponential isotherm model equations.

WSB was brought in contact with the BR2 or OG dyes and was continuously agitated by the use of a power stirrer with impeller blades at 150 rpm for 180 min. During the biosorption process in aqueous solutions at 150 rpm, 0.5 mL of the sample solution was withdrawn from the reactor at pre-determined time intervals, including equilibrium time with the use of micro pipette into 4.5 mL distilled deionized water. At the end of the biosorption period, the sample solutions (5 mL), was centrifuged and all dye concentrations were measure at the absorbance wavelengths (λ_{max}) corresponding to a given dye as shown in Table 1. By the use of standard calibration graph, the amount of dye adsorbed was calculated by differentiating between the dye concentration in solution before and after biosorption process.

The biosorption kinetic data were fitted to Lagergren pseudo-first-order, pseudo-second-order, Elovich, Diffusion-chemisorption, Fractal-like pseudo-first order, Fractal-like pseudo-second order kinetic model equations shown in Table 2.

For repeatability, each experiment was performed twice at least under identical conditions.

Thermodynamic parameters

The effect of temperature on the biosorption process was investigated by dispersing 0.8 g WSB in 300 mL aqueous solutions of BR2 or OG dyes at an initial dye concentration of 50 mg/L and stirred for 180 min at varied temperature. The thermodynamic parameters namely; enthalpy (ΔH°), entropy (ΔS°), and change in the standard free energy (ΔG°), were studied at varied temperatures of 293, 298, 308 and 318 K. The Milonjic thermodynamic parameter correction was applied by which the equilibrium partition constant (k_d) values was multiplied by 1000, to make the constant ' k_d ' dimensionless (Slobodan and Milonjic 2007). These were determined by using following equations;

$$k_d = \frac{C_A}{C_S} \quad (2)$$

$$\Delta G^\circ = -RT \ln(1000)k_d \quad (3)$$

$$\ln k_d = \frac{\Delta S^\circ}{R} - \frac{\Delta H^\circ}{RT} \quad (4)$$

where K_d is the equilibrium partition constant (dimensionless), C_A is the amount of dye adsorbed on the adsorbent of the solution at equilibrium (mg/L), C_S is the equilibrium concentration of the dye in the solution (mg/L). T is the solution temperature (K) and R is the gas constant (8.314 J/mol K). ΔH° and ΔS° were respectively calculated from the slope and intercept of plots of ΔG° versus T .

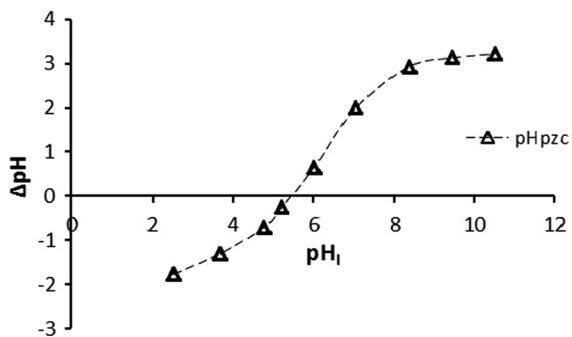
Results and discussion

Characterization of adsorbent

The physicochemical characterization of WSB is shown in Table 1. The pH at point of zero charge (pH_{pzc}) is at 5.45 (Fig. 2). An indication that WSB at $\text{pH} > 5.45$ will facilitate the adsorption of cationic adsorbate while anionic adsorbate adsorption is enhanced at $\text{pH} < 5.45$ (Ma and Eggleton 1999; Mall et al. 2005). The high percentage sample loss on ignition, indicates that WSB is fully carbonaceous material.

Table 2 Adsorption isotherm equation fitted to equilibrium data for the adsorption of BR2 and OG onto WSB

Isotherm models	Non-linear equation	Parameter	References
Langmuir	$q_e = \frac{q_m K_L C_e}{1 + K_L C_e}$	2	Langmuir (1918)
Freundlich	$q_e = K_F C_e^{1/n}$	2	Moon and Lee (1983)
Extended Langmuir	$q_e = \frac{q_m K_L C_e}{1 + K_L C_e + a \sqrt{K_L C_e}}$	3	Chen et al. (2001)
Exponential	$q_e = Q [1 - \exp^{-\beta C_e}]$	2	Shackelford and Daniel (1991)
pseudo-first-order	$q_t = q_e (1 - \exp(-K_1 t))$	2	Lagergren (1898)
pseudo-second-order	$q_t = \frac{k_2 q_e^2 t}{1 + k_2 q_e t}$	2	Ho and McKay (1998)
Elovich	$q_t = \frac{1}{\alpha} \ln(1 + \alpha \beta t)$	2	Low (1960)
Diffusion-chemisorption	$q_t = \frac{1}{\frac{1}{q_e} + \frac{1}{k_{DC} t^{0.5}}}$	2	Sutherland and Venkobachar(2010)
Fractal-like pseudo-first order	$q_t = q_e (1 - \exp(-k_1 t^\alpha))$	3	Brouers and Sotolongo-Costa (2008)
Fractal-like pseudo-second order	$q_t = \frac{k_2 q_e^2 t^\alpha}{1 + k_2 q_e t^\alpha}$	3	Brouers and Sotolongo-Costa (2008)

**Fig. 2** Curve of the pH at point of zero charge (pH_{pzc}) for WSB

Scanning wlectron microscopy (Sem) of WSB morphology

SEM micrograph images of WSB at different magnification showed that WSB particles have a crater-like surface which are heterogeneous nature and some darkish spots which are indications of porosity (Fig. 3a–c). In addition, the Energy Dispersive X-ray (EDX) spectroscopy gave the information of the elemental composition of WSB (Fig. 3d) the EDX revealed the presence of elements such as; C, Na, O, Ca, K, and Mg acting as functional groups which could facilitate the binding of these dye molecules onto the adsorbent's surface.

FTIR spectroscopy study of WSB

Fourier Transformed Infra-Red (FTIR) spectroscopic technique is an important tool for the identification of important functional groups capable of interacting with adsorbate (pollutant ions) in solution. Figure 4 shows the FTIR spectra of WSB before and after being loaded with BR2 and OG dye by biosorption. The spectra were measured within the range of 500–4000 cm^{-1} wavenumber. WSB shows the following observable troughs and peaks at 3371.31, 2920.32, 2852.81, 1647.26, 1373.36, 1035.81, 599.88 and 451.36 cm^{-1} and they were discernibly assigned thus; The broad trough around 3371 cm^{-1} corresponds to –OH stretching vibrations of carboxylic acids, cellulose, pectin and lignin (Yusoff et al. 2014). Two perceptible absorption peaks at the wavenumbers of 2920.32 and 2852.81 cm^{-1} can be assigned to alkyl groups and attributed to –CH stretching vibrations of methyl, methylene and or methoxy groups (Weyer and Lo 2002). Asymmetric vibrations of ionic carboxylic groups (–COO–) appeared at 1647.26 cm^{-1} and the peak at 1373.36 cm^{-1} may be assigned to symmetric stretching of –COO– of pectin. The strong and sharp peak at 1035.81 cm^{-1} is assigned to C–O stretching vibration (Gin et al. 2014). There were significant changes on FTIR spectra of WSB after interaction with the dye molecules (Fig. 4b, c). such is the peaks at 1732.13 and 2123.70 cm^{-1} ; assigned to C=O_{str} originally were on

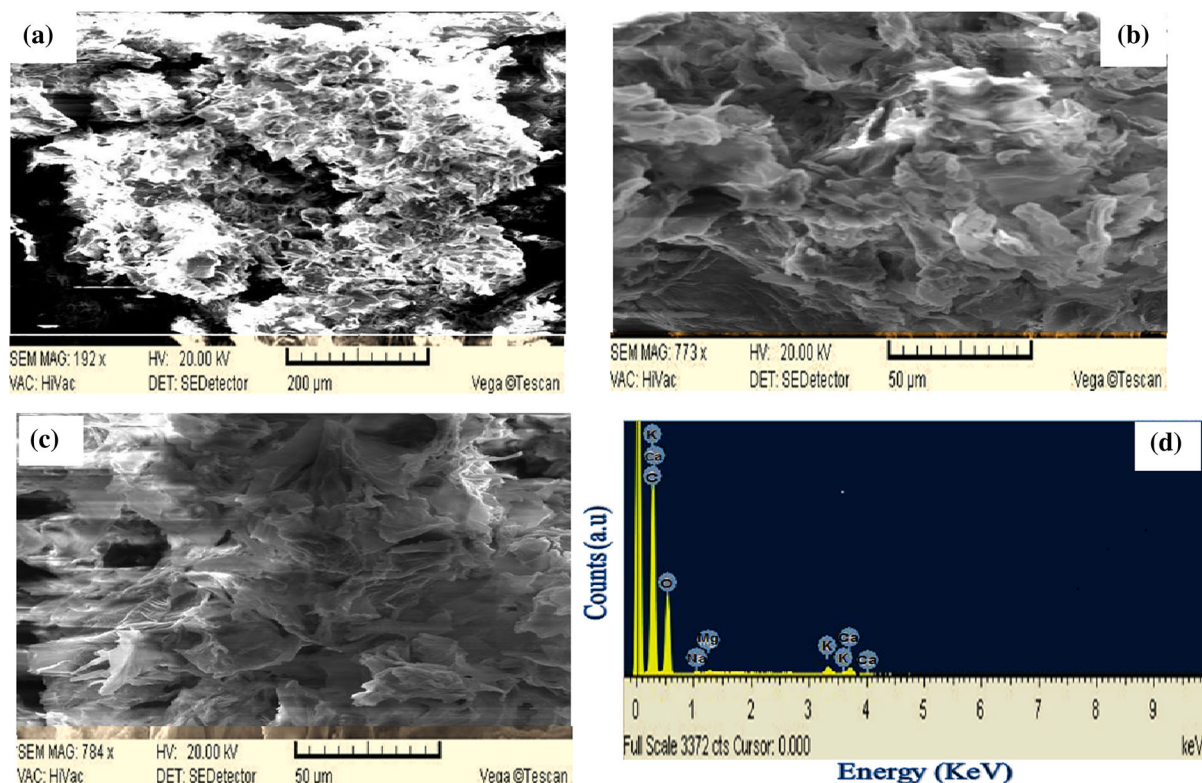


Fig. 3 a–c SEM images of WSB at different magnification and **d** EDX spectrum of WSB

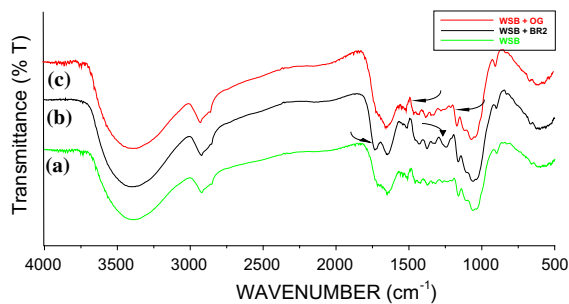


Fig. 4 Fourier transform infrared (FTIR) spectra of **a** OG dye loaded WSB, **b** BR2 dye loaded WSB **c** WSB

the spectra for WSB before biosorption, but disappeared after being loaded with dyes. A new peak appeared on the spectra at 3385.18 cm^{-1} assigned to $\text{NH}_{2\text{str}}$ of the dye molecules following WSB interaction with BR2 or OG dyes. However there were peaks observed unperturbed even after been loaded with dye but instead shifted to a higher frequencies such peaks at 1429.30 cm^{-1} assigned to $\text{CH}_{2\text{str}}$ now shifted to 1456.30 cm^{-1} . The peak at 1244.13 cm^{-1} shifted to 1271.13 cm^{-1} assigned to C-N_{str} on WSB + BR2

spectra (Fig. 4) and the peak at 1159.26 cm^{-1} shifted to 1161.19 cm^{-1} assigned to Ar-N_{str} on WSB + OG spectra. Presumably, the formation of new absorption bands, the change in absorption intensity and the shift in wavenumber of functional groups could be attributed to strong interactions between the dye molecules and binding sites of WSB.

Adsorption experiments

Effect of pH variation

The pH of an aqueous medium is an important factor that may influence the uptake of adsorbate, the effectiveness and efficiency of an adsorbent. Varying the pH of the aqueous medium over the range of between 2 and 11 (Fig. 2), it is observed that the removal of (BR2) from aqueous solution by the biosorbent increases as the pH increases above the PZC value of WSB (at $\text{pH}_{(\text{PZC})} = 5.45$). The percentage of the dye adsorbed was above 95% as the pH tends to an extreme alkaline region. Obviously, the percentage

removal of Orange G (OG) dye by the adsorbent is very high in acidic medium at about pH of 2 (Fig. 5) and as the pH value increases there seems to be a sharp decline in adsorption as it goes higher past pH at the Point of Zero Charge ($pH_{pzc} = 5.45$) (Fig. 5). This implied that when $pH = pH_{pzc}$, the surface charge of adsorbents is neutral, and a kind of negligible electrostatic attraction exists between the adsorbent and the dye molecules (either BR2 or OG) in solution. However, as pH goes below the pH_{pzc} , the surface charge of WSB becomes positively charged and enhances the interaction of OG (anionic) to WSB and inhibits the approach of positively charged cations. While on the other way round according to Rivera-Utrilla et al. (2013), an increase in the negative surface charge of the adsorbent enhances the adsorption of positively charged species. Hence at pH greater than pH_{pzc} , the surface charge of WSB is negative (Adedirin et al. 2011), thus, the adsorption of BR2 (cationic) onto WSB is favoured. Therefore, in this study the pH of OG was adjusted and maintained around $pH \approx 2$. While for maximum removal of BR2 the pH was used naturally without any adjustment since the natural pH of BR2 in solution is above the point of zero charge value.

Biosorbent dose variation

The doses of WSB added to constant BR2 and OG dye solution concentrations were varied to quantify and establish adsorption capacity of WSB at the same temperature and pH conditions. Apparently as the dosage of WSB increases from 0.007 to 0.5 g, the amount of BR2 and OG dye adsorbed per unit mass, decreases (Fig. 6). It is readily understood that the number of available adsorption sites increases by increasing the adsorbent dose. According to Omorogie

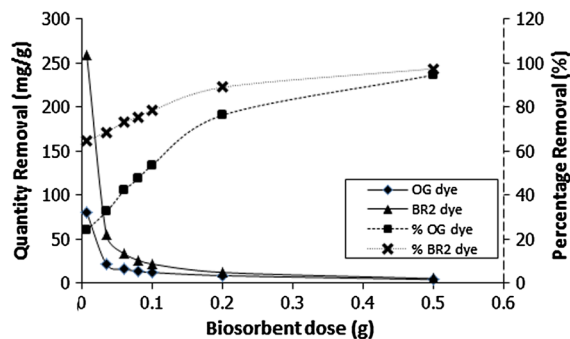


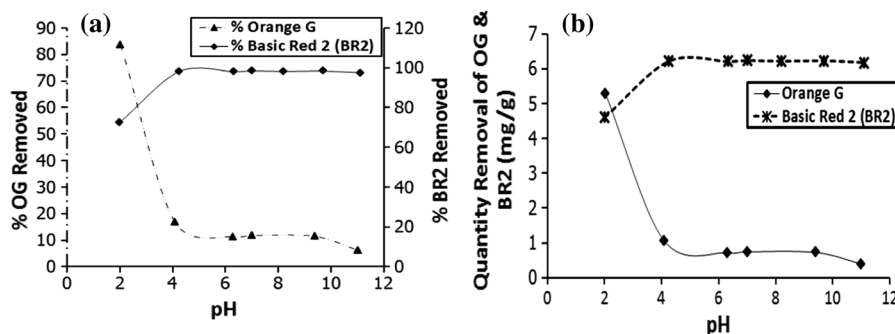
Fig. 6 Biosorbent dosage variation for the uptake of Orange G (OG) and Basic red (BR2) onto WSB

et al. (2016), increase in the mass of biosorbent dose will lead to a decrease in the amount of BR2 and OG biosorbed by WSB due to the aggregation/agglomeration of biosorbent particles and probably bring about blockage of biosorption sites which at the long run could lead to decrease in surface area, decrease in sorbate–sorbent interaction and lengthening of diffusion path length.

Biosorption equilibrium

Adsorption equilibrium is the ratio of the amount of adsorbate adsorbed to the amount remaining in solution, established when it has been in contact with an adsorbent for sufficient period of time. While the description of the retention, release or even the mobility of the adsorbate from aqueous porous media or aquatic environment to an adsorbent at a constant temperature and pH is by the use of an invaluable curve known as adsorption isotherm. According to Bulut et al. (2008), the physicochemical parameters together with the underlying thermodynamic assumptions provide an insight into the adsorption mechanism, surface properties as well as the degree of

Fig. 5 Effect of pH variation for the adsorption of BR2 and OG onto watermelon shell Biosorbent (WSB)



affinity of the adsorbent of interest (Omorieg et al. 2016).

In this study nonlinear regression was used to compare the fitting of isotherm models; the Langmuir, Freundlich, extended Langmuir and exponential isotherm models (Table 2). These isotherm models were statistically appraised using three well known goodness-of-fit parameters namely square of correlation coefficient (r^2) variance (σ^2) and Chi square test (χ^2).

In a proposed single component system of biosorption, there is a possibility that the aqueous environment may contain more than one type of adsorbate (impurities/components) even in the presence of the main and preferred adsorbate (dye). The implication is then that when several components are present, interference and competition for biosorbent sites occur and may lead to a complex mathematical formulation for the equilibrium system. Hence, the Extended Langmuir Isotherm (ELI) a three parameter model is appropriate to investigate this phenomenon (Chen et al. 2001). However, like Langmuir isotherm model, the ELI (a predictive model) assumes a homogeneous surface with respect to the energy of adsorption, no interaction between adsorbed species, and that all sites are equally available to all adsorbed species. As shown in Fig. 7, the ELI accurately describes the sorption behaviour of both BR2 and OG dyes onto WSB. The fitting of ELI to the equilibrium data is confirmed examining the isotherm constants alongside their goodness-of-fit as shown in Tables 2 and 3. This implied that there is a homogenous site within the Biosorbent (WSB) and the biosorption of both dyes is by chemisorption.

Biosorption kinetic studies

Sorption kinetics is expressed as the solute rate that controls the residence time of the adsorbate in the

solid-solution interface. Few kinetic models were applied to fit the sorption process in this study, namely; two parameter kinetic models such as pseudo-first (Lagergren 1898) and pseudo-second-order model (Ho and McKay 1998), Elovich (Low (1960)) and Diffusion–chemisorption (Sutherland and Venkobachar 2010) kinetics and three parameter models; fractal-like pseudo-first order and fractal-like pseudo-second order kinetics (Brouers and Sotolongo-Costa 2008) as shown in Table 2. In this study, nonlinear regression was used to determine the best-fit kinetic model's rate equation. Contrary to the linearization models, nonlinear regression usually involves the minimization or maximization of error distribution (between the experimental data and the predicted) based on its convergence criteria (Kumar et al. 2008).

Undoubtedly, linear regression analysis has frequently been employed in accessing the quality of fits and adsorption performance (Kundu and Gupta 2006), primarily owing to its wide usefulness in a variety of adsorption data (Rivas et al. 2006) and partly reflecting the appealing simplicity of its equations (Ayoob and Gupta 2008). However, during the last few years, interest in the utilization of nonlinear optimization modeling has been noted (Prasad and Srivastava 2009).

Therefore in this study, by nonlinear regression plots, goodness of conformity between experimental data and the model-predicted values was evaluated with emphases on the coefficient of determination (R^2), Variance (σ^2) and the Chi square test (χ^2). Observably, the Pseudo-first-order and Pseudo-second-order kinetic models did not fit the experimental data for the adsorption process of both adsorbate (i.e. BR2 and OG) adsorbed onto WSB (Fig. 8a, b) while Fig. 9a, showed that Elovich kinetic model fitted very well to BR2 biosorption kinetic data and Diffusion–

Fig. 7 Equilibrium Isotherm non-linear plot for the fit of four different models to **a** OG dye adsorption experiment data and **b** BR2 dye adsorption experiment data after been adsorbed onto WSB

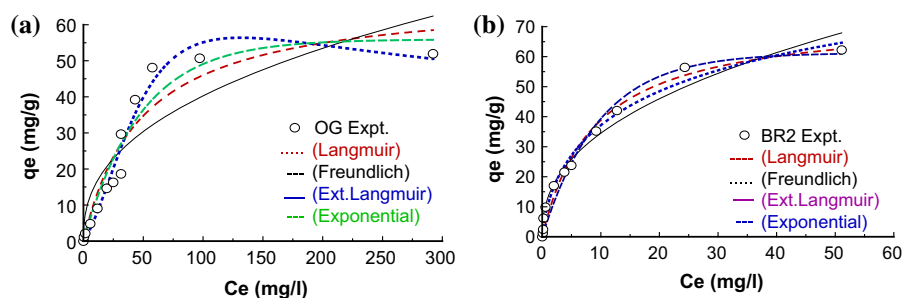


Table 3 Comparison of nonlinear regression data for different equilibrium isotherm models for the adsorption of OG and BR2 dye onto WSB

	Isotherm constant (OG)	Goodness-of-fit (OG)			Isotherm constant (BR2)	Goodness-of-fit (BR2)				
		R ²	σ ²	χ ²		R ²	σ ²	χ ²		
Langmiur	q _m (mg/g)	68.14	0.9111	37.41	17.13	q _m (mg/g)	73.53	0.9833	8.50	8.39
	K _L (L/g)	0.02				K _L (L/g)	0.11			
Freundlich	K _F (L/g)	6.15	0.8078	80.91	60.13	K _F (L/g)	13.24	0.9743	13.08	20.59
	N	2.45				n	2.41			
Exponential	Q	55.93	0.9395	25.48	12.60	q	61.24	0.9767	11.83	11.64
	β	0.02				β	0.10			
Extended Langmiur	q _m (mg/g)	27.24	0.9703	13.8	7.54	q _m (mg/g)	125.79	0.9886	6.44	3.52
	K _L (L/g)	0.01				K _L (L/g)	0.22			
	a	−1.44				a	2.91			

Fig. 8 Plot of the pseudo-first and pseudo-second order adsorption kinetics of **a** BR2 dye and **b** OG dyes onto WSB at different initial dye concentrations

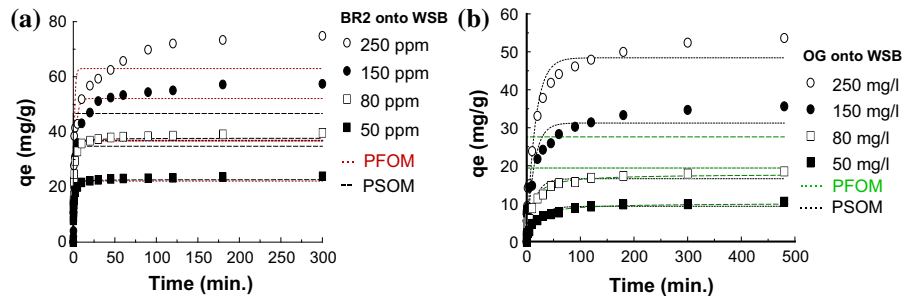
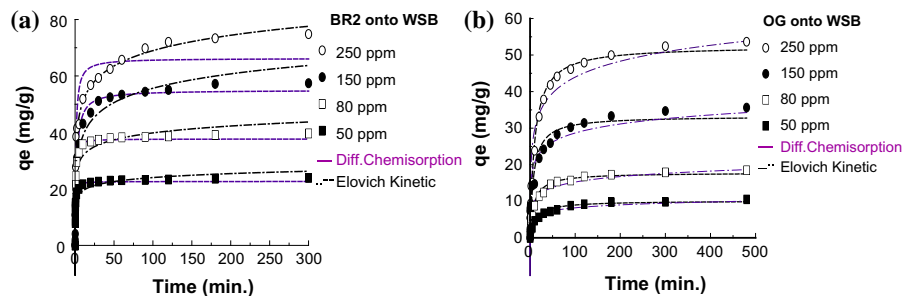


Fig. 9 Plot of the diffusion–chemisorption and Elovich adsorption kinetics of **a** BR2 dye and **b** OG dyes onto WSB at different initial dye concentrations



chemisorption kinetic model fitted well to OG equilibrium (Fig. 9b).

Meanwhile, Fig. 10a, b shows the plot for the three parameter model of Fractal-like Pseudo-first order which gave very satisfactory fit for both BR2 and OG dyes as against Fractal-like Pseudo-second order kinetic which could not satisfactorily explain the sorption mechanism for both dyes.

Two parameters goodness of FIT

Elovich model provided very satisfactory fits for the equilibrium data for the adsorption of BR2 (cationic dye) onto WSB. The highest values of the correlation coefficient (R²) (0.9840–0.9582) and the least values of the variance and Chi square test confirmed the goodness of fit of the model (Table 4 and Fig. 9a, b). According to Low (1960), Elovich model basically

Fig. 10 Plot of the fractal-like pseudo-first order and Fractal-like pseudo-second order kinetics of **a** BR2 dye and **b** OG dyes onto WSB at different initial dye concentrations

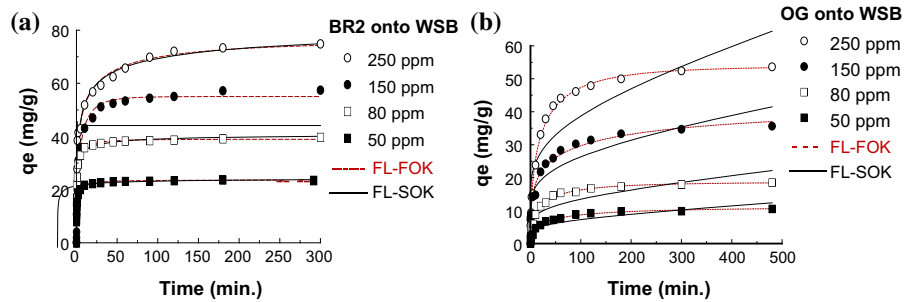


Table 4 The comparison of the sorption rate of BR2 dye onto WSB using different kinetic models alongside goodness-of-fit statistical parameters

pseudo-first order model (PFOM)						pseudo-second order model (PSOM)						
Co (mg/L)	q _e	K ₁	R ²	σ ²	χ ²	q _e	K ₂	R ²	σ ²	χ ²		
50	22.160	1.840	0.8620	7.73	12.16	22.668	0.147	0.9291	3.97	161.35		
80	36.816	1.600	0.8849	18.63	18.93	37.714	0.074	0.9418	9.42	122.95		
150	52.081	0.392	0.9660	18.04	8.78	34.765	-3.6×10^4	0.1346	458.49	146.63		
250	62.953	0.786	0.8792	78.36	36.14	46.666	-3.2×10^4	0.1982	520.03	7496.89		
Elovich kinetic model (EKM)					Diffusion–chemisorption kinetics model (DCM)							
Co (mg/L)	β	α	R ²	σ ²	χ ²	q _e	K _{CD}	R ²	σ ²	χ ²		
50	2.030	679.401	0.9598	2.25	1.98	75.381	22.668	0.9291	3.97	6.64		
80	3.519	235.274	0.9582	6.76	3.72	105.393	37.714	0.9418	9.42	10.45		
150	7.343	2.669	0.9777	11.81	43.45	29.012	55.018	0.9917	4.41	3.09		
250	7.843	8.424	0.9840	10.39	8.28	65.754	66.261	0.9316	44.35	23.59		
Fractal-like PFOM						Fractal like PSOM						
Co (mg/l)	q _e	K ₁	α	R ²	σ ²	χ ²	q _e	K ₂	α	R ²	σ ²	χ ²
50	23.594	1.036	0.352	0.9931	0.41	0.63	25.225	0.063	0.479	0.9892	0.65	0.96
80	38.970	0.991	0.376	0.9936	1.11	1.09	41.501	0.036	0.512	0.9900	1.73	1.69
150	55.046	0.421	0.573	0.9900	5.62	31.94	44.132	-7.5×10^5	23.045	0.6978	170.78	117.09
250	76.480	0.509	0.341	0.9845	10.70	5.89	86.283	0.007	0.431	0.9865	9.32	5.12

explains the chemisorptive nature of interaction of the cationic dye with active sites on the surface of WSB.

Diffusion–chemisorption kinetic model provided very satisfactory fit for the equilibrium data for the adsorption of OG (anionic dye) onto WSB. The correlation coefficient (R²) provided by this model is highest with respect to other model in the range of 0.9749–0.8874 (Table 5) and this was further established by the least values of variance and Chi square test. According to Sutherland and Venkobachar (2010), the diffusion–chemisorption model implies

that the rate of occupation of biosorbent sites by adsorbate ions is not only a function of unoccupied sites but also the structure of the biosorbent. This therefore implied that the rate of occupation of the active sites on WSB by OG dye was by chemisorption and by diffusion of the OG dye particle into the crevice of WSB.

Table 5 The comparison of the kinetics of OG sorption onto WSB using two parameter kinetic model alongside goodness-of-fit parameters

pseudo-first order model (PFOM)						Pseudo-second order model (PSOM)						
Co (mg/L)	q _e	K ₁	R ²	σ ²	χ ²	q _e	K ₂	R ²	σ ²	χ ²		
50	9.302	0.051	0.9255	1.07	7.93	10.119	0.008	0.9567	0.62	871.10		
80	16.558	0.071	0.9397	2.96	11.02	17.795	0.006	0.9688	1.53	154.04		
150	31.228	0.074	0.8395	23.28	41.91	19.375	-7.3 × 10 ⁴	0.1442	124.18	65.21		
250	48.412	0.064	0.9528	19.66	30.28	27.573	-2.2 × 10 ⁴	0.1017	374.27	29.16		
Elovich kinetic model (EKM)						Diffusion–chemisorption kinetics model (DCM)						
Co (mg/L)	β	α	R ²	σ ²	χ ²	q _e	K _{CD}	R ²	σ ²	χ ²		
50	1.156	10.511	0.9391	0.87	9.56	0.792	10.119	0.9567	0.62	5.82		
80	2.163	5.342	0.9617	1.88	19.30	2.027	17.795	0.9688	1.53	7.03		
150	3.565	8.738	0.9296	10.21	18.12	4.264	33.289	0.8874	16.34	32.64		
250	6.283	1.741	0.9514	20.25	62.50	5.104	52.482	0.9749	10.45	21.18		
Fractal-like PFOM						Fractal like PSOM						
Co (mg/l)	q _e	K ₁	α	R ²	σ ²	χ ²	q _e	K ₂	α	R ²	σ ²	χ ²
50	11.063	0.190	0.455	0.9924	0.12	0.76	0.145	-7.230	-0.005	0.8659	2.05	17.60
80	18.628	0.215	0.492	0.9946	0.28	1.09	0.259	-4.026	-0.005	0.8366	8.51	70.64
150	43.063	0.255	0.331	0.9819	2.79	4.45	0.752	-1.413	-0.007	0.9006	15.33	17.35
250	53.820	0.195	0.518	0.9947	2.34	2.80	0.780	-1.341	-0.005	0.8340	73.48	169.91

Three parameter goodness of FIT

According to Brouers and Sotolongo-Costa (2008), fractal-like kinetic formula, two major parameters (n , α) are been considered. Where ' α ' is the fractional time index and ' n ' is the non-integer order of reaction. These two parameters has been fitted to a few problems of fundamental and practical importance, in particular, the sorption of dissolved contaminants in liquid phase (Jurlewicz and Weron 1999). For special values of the two parameters n and α , some typical resolutions are arrived at (Jurlewicz and Weron 1999; Brouers and Sotolongo-Costa (2008) which includes: (a) If $n = 1$; $\alpha = 1$, which describes the rate function of the process as a first-order kinetic. (b) If $n = 1$; $\alpha \neq 1$, it introduces a function by Picoli et al. (2003) known as "Weibull kinetics" implying that either $0 < \alpha < 1$, is a "stretched exponential kinetic" or $\alpha > 1$, is a "squeezed exponential" (c) If $n = 2$, $\alpha = 1$, describes the rate function of the process as a second-order kinetic and (d) If $n = 2$, $\alpha \neq 1$; gives a generalized second-order kinetic for such process. Hence as shown

(Fig. 10a, b and Tables 4 and 5), Fractal-like pseudo First-order kinetic equation satisfactorily fit to both kinetic data for BR2 and OG dyes than the Fractal-like pseudo second-order kinetic equation for the uptake of the dyes onto WSB. The fractional time index ' α ' has values in the range of 0.46–0.52 (i.e. $0 < \alpha < 1$) (Tables 4 and 5) meaning that $n = 1$, which then explains that the mechanism of adsorption of both dyes to be stretched exponential kinetic of the Fractal-like pseudo first kinetics. This in addition corroborate the earlier kinetic model fitting by Elovich and Diffusion chemisorption that the adsorbate-adsorbent interaction has been by chemical reaction through chemisorption following the path of simple exponential decay of the dyes from the bulk solution onto WSB. The values of correlation coefficient (R^2) (0.9840–0.9582), the least values of the variance and Chi square test accented to this as shown in Tables 4 and 5.

Table 6 Thermodynamic parameters for the adsorption of BR2 and OG onto WSB

Biosorbent	Dye	ΔG° (KJ/mol)				ΔH° (KJ/mol)	ΔS° (J/mol/k)
		293 K	298 K	308 K	318 K		
WSB	BR2	-23.622	-22.946	-22.383	-21.229	0.090	-50.036
	OG	-22.390	-22.844	-24.729	-24.729	-0.94	5.127

Thermodynamic parameters

The thermodynamic parameters ΔG° , ΔH° and ΔS° were determined using Eqs. 2, 3 and 4 modified with equilibrium partition constant (k_d), dimensionless parameter correction factor (Slobodan and Milonjic2007). As shown in Table 6, the values of the free energy (ΔG°) were negative, indicating that the adsorption reaction was spontaneous within the temperatures studied. It is also observable (Table 6) that as the temperature was increased (293–318 K), the negative ΔG° values for the uptake of OG onto WSB also increased, an indication that the spontaneity of the adsorption reaction increases with rise in temperature. Whereas, this was the opposite in the case of the uptake of BR2 onto WSB, where there was decrease in spontaneity with rise in temperature.

The positive value for the enthalpy change, ΔH° (0.090 kJ/mol) for BR2 adsorption, indicates the endothermic nature of the adsorption, which implies that the heat of reaction was absorbed externally into the system and brings about an increase in BR2 adsorption efficiency as the temperature increases. While the negative value for the enthalpy change, ΔH° (-0.094 kJ/mol) for OG dye onto WSB is an indication that the adsorption was exothermic in nature meaning that there was an evolution of heat to the environment from the system. It also indicates that the process of adsorption of OG dye is energetically stable (Horsfall et al. 2004).

The positive value for the entropy change, ΔS° (5.127 J/mol K), indicates an increased disorderliness at the solid–liquid interface during OG dye adsorption onto the WSB whereas the negative value for the entropy change, ΔS° (-50.036 J/mol K), indicates a less disorderliness at the solid-liquid interface during BR2 dye adsorption.

Conclusion

Watermelon shell biosorbent (WSB) used in this work, indicated that it can be used as a low cost sorbent for the sorption of anionic and cationic dye contaminants from aqueous solution. The physicochemical characteristics and surface morphology of WSB was determined and it showed that it had varieties of atoms that can interact with substrates by sharing or transfer of electrons. The equilibrium data satisfactorily fit to Extended Langmuir isotherm model. The amounts of both dyes adsorbed by WSB are 125 mg/g for BR2 and 27 mg/g for OG. Various models showed that the mechanism of reaction between the dye molecules and WSB was by chemisorption. First were the Fractal-like pseudo-first order kinetic model parameters, which revealed that the rate limiting step for the interaction of both dye with WSB was by stretched exponential decay. Second was the satisfactory fit of the kinetic data to Elovich and Diffusion–Chemosorption models for BR2 and OG dyes onto WSB respectively. All these models pointed to the fact that the mechanisms of interaction between WSB and the dyes are either by bond formation or electrostatic attraction. Biosorption of the dye molecules onto the biosorbent was spontaneous going by the negative values of the free energy (ΔG°). However, there was a distinction in the values of ΔH° such that the adsorption process of BR2 was endothermic and that of OG exothermic, while the entropy of adsorption (ΔS°) showed that the adsorbate-adsorbent interaction between OG and WSB was more random than between BR2 and WSB.

References

- Adedirin O, Adamu U, Nnabuk EO (2011) Removal of Cd(II) from aqueous solution using *Bacillus subtilis* and *Escherichia coli* immobilized in agarose gel: equilibrium kinetics and thermodynamic study. *Arch Appl Sci Res* 3(3):59–76
- Ayoob S, Gupta AK (2008) Insights into isotherm making in the sorptive removal of fluoride from drinking water. *J Hazard Mater* 152:976–985
- Babalola JO, Koiki BA, Eniyawu Y, Salimonu A, Olowoyo A, Oninla VO, Alabi HA, Ofomaja AE, Omorogie MO (2016a) Adsorption efficacy of *Cedrela odorata* seed waste for dyes: non linear fractal kinetics and non linear equilibrium studies. *J Environ Chem Eng* 4(3):3527–3536
- Babalola JO, Olowoyo JO, Durojaiye AO, Olatunde AM, Unuabonah EI, Omorogie MO (2016b) Understanding the removal and regeneration potentials of biogenic wastes for toxic metals and organic dyes. *J Taiwan Inst Chem Eng* 58:490–499
- Banerjee K, Ramesh ST, Gandhimathi R, Nidheesh PV, Bharathi KS (2012) A Novel agricultural waste adsorbent, watermelon shell for the removal of copper from aqueous solutions. *Iran J. Energy Environ* 3(2):143–156
- Barka N, Abdennouri M, Boussaoud A, Makhfouk M-EI (2010) Biosorption characteristics of Cadmium (II) onto *scolymus hispanicus* as low-cost natural biosorbent. *Desalination* 258:66–71
- Bhattacharya AK, Naiya TK, Mondal SN, Das SK (2008) Adsorption, kinetics and equilibrium studies on removal of Cr (VI) from aqueous solutions using different low-cost adsorbents. *Chem Eng J* 137:529–541
- Brouers F, Sotolongo-Costa O (2008) Generalized fractal kinetics in complex systems (application to biophysics and biotechnology). *Physica A Stat Mech Appl* 368:165–175
- Bulut Y, Tez Z (2007) Adsorption studies on ground shells of Hazelnut and Almond. *J Hazard Mater* 149:35–41
- Bulut E, Ozacar M, Sengil IA (2008) Adsorption of malachite green onto bentonite: equilibrium and kinetic studies and process design. *Micropor Mesopor Mater* 115:234–246
- Chen B, Hui CW, McKay G (2001) Film-pore diffusion modelling for the sorption of metal ions from aqueous effluents onto peat. *Water Res* 35:3345–3356
- Depci T, Kul AR, Onal Y (2012) Competitive adsorption of Lead and Zinc from aqueous solution on activated Carbon prepared from van apple pulp: study in single- and multi-solute systems. *Chem Eng J* 200–202:224–236
- Gin WA, Jimoh A, Abdulkareem AS, Giwa A (2014) Production of activated carbon from watermelon peel. *Int J Sci Eng Res* 5(2):66–71
- Gupta VK, Nayak A (2012) Cadmium removal and recovery from aqueous solutions by novel adsorbents prepared from orange peel and Fe₂O₃ nanoparticles. *Chem Eng J* 180:81–90
- Gupta VK, Mittal A, Gajbe V (2005) Adsorption and desorption studies of water soluble dye, Quinoline Yellow, using waste materials. *J Coll Interf Sci* 284:89–98
- Hameed BH, Ahamad AA (2009) Batch adsorption of methylene blue from aqueous solution by garlic peel, an agricultural waste biomass. *J Hazard Mater* 164:3115–3121
- Hameed BH, El-Khaiary MI (2008) Kinetics and equilibrium studies of Malachite green adsorption on rice straw-derived char. *J Hazard Mater* 153:701–708
- Ho Y, McKay GA (1998) Comparison of chemisorption kinetic models applied to pollutant removal on various sorbents. *Process Saf Environ Prot* 76:332–340
- Horsfall M, Spiff AI, Abia AA (2004) Studies on the influence of mercaptoacetic acid (maa) modification of cassava (manihot sculentacranz) waste biomass on the adsorption of Cu²⁺ and Cd²⁺ from aqueous solution. *Bull Korean Chem Soc* 25:969–976
- Husein DZ, Aazam E, Battia M (2017) Adsorption of cadmium(II) onto watermelon rind under microwave radiation and application into surface water from Jeddah, Saudi Arabia Arabian. *J Sci Eng* 42:2403–2415. doi:10.1007/s13369-016-2381-2
- Iqbal M, Saeed A, Zafar SI (2009) FTIR spectrophotometry, kinetics and adsorption isotherms modeling, ion exchange, and EDX analysis for understanding the mechanism of Cd²⁺ and Pb²⁺ removal by mango peel waste. *J Hazard Mater* 164:161–171
- Jurlewicz A, Weron KA (1999) General probabilistic approach to the universal relaxation response of complex systems. *Cell Mol Biol Lett* 1(04):55–86
- Kanawade SM, Gaikwad RW (2011) Removal of zinc ions from industrial effluent by using cork powder as adsorbent. *Int J Chem Eng Appl* 2:199–201
- Kiruba UP, Senthil Kumar P, Prabhakaran C, Aditya V (2014) Characteristics of thermodynamic, isotherm, kinetic, mechanism and design equations for the analysis of adsorption in Cd (II) ions-surface modified eucalyptus seeds system. *J Taiwan Inst Chem* 45:2957–2968
- Kumar KV, Porkodi K, Rocha F (2008) Isotherms and thermodynamics by linear and non-linear regression analysis for the sorption of methylene blue onto activated carbon: comparison of various error functions. *J Hazard Mater* 151:794–804
- Kundu S, Gupta AK (2006) Arsenic adsorption onto iron oxide-coated cement (iocc): regression analysis of equilibrium data with several isotherm models and their optimization. *Chem Eng J* 122:93–106
- Lagergren S (1898) Zurtheorie der sogenannten adsorption gelosterstoffe. *K Sven VetenskapsakadHandl* 24:1–39
- Lakshmipathy R, Sarada NC (2013) Application of watermelon rind as sorbent for removal of nickel and cobalt from aqueous solution. *Int J Miner Process* 122:63–65
- Langmuir I (1918) The adsorption of gases on plane surface of glass, mica and platinum. *J Am Chem Soc* 40:1361–1403
- Lashee MR, Ammar NS, Ibrahim HS (2012) Adsorption/desorption of Cd(II), Cu(II) and Pb(II) using chemically modified orange peel: equilibrium and kinetic studies. *Solid State Sci* 14:202–210
- Low MJD (1960) Kinetics of chemisorption of gases on solids. *Chem Rev* 60:267–312
- Ma C, Eggleton RA (1999) Cation exchange capacity of kaolinite. *Clays Clay Miner* 47:174–180
- Mall ID, Srivastava VC, Agarwal NK, Mishra IM (2005) Removal of congo red from aqueous solution by bagasse fly ash and activated carbon: kinetic study and equilibrium isotherm analyses. *Chemosphere* 61:492–501
- Moon H, Lee WK (1983) Intraparticle diffusion in liquid phase adsorption of phenols with activated carbon in a finite batch adsorber. *J Colloid Interface Sci* 96(1):162–170

- Mushtaq M, Bhatti HN, Iqbal M, Noreen S (2016) *Eriobotrya Japonica* seed biocomposite efficiency for Copper adsorption: isotherms, kinetics, thermodynamic and desorption studies. *J Environ Manag* 176:21–33
- Nandi BK, Goswami A, Purkait MK (2009) Removal of cationic dyes from aqueous solutions by kaolin: kinetic and equilibrium studies. *Appl Clay Sci* 42:583–590
- Ogobodu RO, Omorogie MO, Unuabonah EI, Babalola JO (2015) Biosorption of heavy metals from aqueous solutions *Parkia biglobosa* biomass: equilibrium, kinetics, and thermodynamic studies. *Environ Prog Sustain Energy* 34(6):1694–1704
- Oladoja NA, Aliu YD (2008) Snail shell as coagulant aid in the alum precipitation of malachite green from aqua system. *J Hazard Mater* 67:114–120
- Oladoja NA, Aliu YD (2009) Snail shell as coagulant aid in the alum precipitation of malachite green from aqua system. *J Hazard Mater* 164:1494–1502
- Omorogie MO, Babalola JO, Unuabonah EI, Gong JR (2012) Kinetics and thermodynamics of heavy metal ions sequestration onto novel *Nauclea diderrichii* seed biomass. *Bioresour Technol* 118:576–579
- Omorogie MO, Babalola JO, Unuabonah EI, Gong JR (2014) Hybrid materials from agro waste and nanoparticles: implications on the kinetics of the adsorption of inorganic pollutants. *Environ Technol* 35(5):611–619
- Omorogie MO, Babalola JO, Unuabonah EI, Song W, Gong JR (2016) Efficient chromium abstraction from aqueous solution using a low-cost biosorbent: *Nauclea diderrichii* seed waste. *J Saudi Chem Soc* 20(1):49–57
- Paraskeva P, Kalderis D, Diamadopoulos E (2008) Production of activated carbon from agricultural by-products. *J Chem Technol Biotechnol* 83:581–592
- Picoli S, Mendes RS, Malacarne LC (2003) Q-exponential, Weibull, and q-Weibull distributions: an empirical analysis. *Physica A: Stat Mech Appl* 324(3):678–688
- Prasad RK, Srivastava SN (2009) Sorption of distillery spent wash onto fly ash: kinetics and mass transfer studies. *Chem Eng J* 146(1):90–97
- Rashid A, Bhatti HN, Iqbal M, Noreen S (2016) Fungal biomass composite with bentonite efficiency for Nickel and Zinc adsorption: a mechanistic study. *Ecol Eng* 91:459–471
- Rivas FJ, Beltran FJ, Gimeno O, Frades J, Carvalho F (2006) Adsorption of landfill leachates onto activated carbon equilibrium and kinetics. *J Hazard Mater* B131:170–178
- Rivera-Utrilla J, Gómez-Pacheco CV, Sánchez-Polo M, López-Peñalver JJ, Ocampo-Pérez R (2013) Tetracycline removal from water by adsorption/bioadsorption on activated carbons and sludge-derived adsorbents. *J Environ Manage* 131:16–24
- Saeed A, Iqbal M, Holl WH (2009) Kinetics, equilibrium and mechanism of Cd²⁺ removal from aqueous solution by Mung bean husk. *J Hazard Mater* 168:1467–1475
- Shackelford CD, Daniel DE (1991) Diffusion in saturated soil I: background, American society of civil engineers. *J Geotech Eng* 117(3):467–484
- Slobodan K, Milonjić A (2007) Consideration of the correct calculation of thermodynamic parameters of adsorption. *J Serbian Chem Soc* 72(12):1363–1367
- Suteu D, Zaharia C, Muresan A, Muresan R, Popescu A (2009) Using of industrial waste materials for textile wastewater treatment. *Environ Eng Manag J* 8:1097–1102
- Sutherland C, Venkobachar AC (2010) Diffusion-chemisorption kinetic model for simulating biosorption using forest macro-fungus, *Fomes fasciatus*. *Intl Res J Plant Sci* 1(4): 107–117
- Tahir MA, Bhatti HN, Iqbal M (2016) Solar red and brittle blue direct dyes adsorption onto *Eucalyptus angophoroides* bark: equilibrium, kinetics and thermodynamic studies. *J Environ Chem Eng* 4:2431–2439
- Unuabonah EI, Adedapo AO, Nnamdi CO, Adewuyi A, Omorogie MO, Adebowale KO, Olu-Owolabi BI, Ofomaja AE, Taubert A (2015) Successful scale-up performance of a novel papaya-clay combo adsorbent: up-flow adsorption of a basic dye. *Desalin Water Treat* 56(2):536–551
- Weyer LG, Lo SC (2002) Spectra-structure correlations in the near-infrared. In handbook of vibrational spectroscopy. Wiley UK 91(3):631–639
- Yang S, Chen C, Chen Y, Li J, Wang D, Wang X, Hu W (2015) Competitive adsorption of Pb II, Ni II, and Sr II ions on grapheme oxides: a combined experimental and theoretical study. *ChemPlus Chem* 80:480–484
- Yusoff SNM, Kamari A, Putra WP, Ishak CF, Mohamed A, Hashim N, Md Isa I (2014) Removal of Cu(II), Pb(II) and Zn(II) ions from aqueous solutions using selected agricultural wastes: adsorption and characterisation studies. *J Environ Pro* 5:289–300. doi:10.4236/jep.2014.54032
- Yuvaraja G, Krishnaiah N, Subbaiah MV, Krishnaiah A (2014) Biosorption of Pb(II) from aqueous solution by *solanum melongena* leaf powder as a low-cost biosorbent prepared from agricultural waste. *Colloids Surf B* 114:75–81
- Zaharia C, Suteu D, Muresan A, Muresan R, Popescu A (2009) Textile wastewater treatment by homogenous oxidation with hydrogen peroxide. *Environ Eng Manag J* 8(6):1359–1369